

Chapter VII

*Molecular dynamics simulation
of human bifunctional glutamyl-
prolyl-tRNA synthetase*

7.1: Introduction

Aminoacyl -tRNA synthetases catalyze the attachment of amino acids to their specific tRNAs in protein synthesis. They are also involved in various biological processes. In higher eukaryotes several of these enzymes are found in a multienzyme complex [1-4]. These multiprotine complexes are composed by nine synthetases (IRS, LRS, MRS, QRS, PRS, KRS, DRS, and bifunctional EPRS) and three auxiliary proteins p18, p38, p43 [5, 6]. These nine synthetases react with Glu, Pro, Ile, Leu, Met, Lys, Gln, Arg, Asp [7]. With the tRNA synthetase of higher eukaryotes, glutamyl and prolyl - tRNA synthetase of higher eukaryotes catalytic activities have been found linked in a single polypeptide [8, 9]. In human glutamyl - prolyl - tRNA synthetase (EPRS), two catalytic domains exhibiting each enzyme activity are linked by a linker peptide that contains three tandemly repeated motifs (EPRS-R1, EPRS-R2, EPRS-R3) of 57 amino acids [9]. In human prolyl - tRNA synthetase absent of this linker peptide was still active, suggesting that it is not essential for catalytic activity. Therefore linker region may play a different role in the cell other than the catalytic function [10]. Peptide sequences homologous to these repeats have also been found in other tRNA synthetases. They are present as a single copy in the N-terminal extensions of glycyl, tryptophanyl, histidyl tRNA synthetases, which have been found as free forms and in the C-terminal extension methionyl t-RNA synthetase has been found in the complex form (11-15). These motifs were identified as an antigenic epitope for auto antibodies detected in myositis patients (16). In Human histidyl-t RNA synthetase due to the lacking of this peptide region it is lost antigenicity and catalytic activities, suggesting its importance in these two activities (17). EPRS-R1 contain helix-turn-helix structural motif (18). Jeong et al. solved the NMR structure of multifunctional peptide motifs in human bifunctional glutamyl-prolyl-tRNA synthetase [19]. Two helices are found in residues from 679 to 699 and from 702 to

721. Two helices are interacting with hydrophobic residues [Val (692), Leu (695), Ala (670), Val (705), and Ala (708)] close to turn involved in helix-helix interaction. The C-terminal loop folds back to interact with the aromatic residues. The hydrophobic interaction between Tyr (727) in the loop Tyr (682), Tyr (719) in the helix are essential for the C-terminal loop formation. Also hydrophobic residues are involved in helix-helix interaction but other are on the surface. These suggest that they may in role in protein-protein or protein-nucleic acid interaction. When non catalytic motifs attached to the catalytic domains of tRNAsynthetase including the repeated motifs of EPRS, exert biological function. One is that they are involved in protein-protein interaction for the multi-tRNAsynthetase complex and another is that they used as a tRNA-binding motif for delivery and efficiency. The RNA binding mode of this helix- turn-helix motifs also found in other homologous RNA binding motifs and used in protein RNA interaction. Repetition of helix-turn-helix to enhanced functional flexibility and binding affinity in molecular interaction.

In this work we intend to obtain the motional properties of protein, its secondary structure and important residues by monitoring RMSD, Radius of gyration and also through principal component analysis.

7.2: Materials and Methods

Solution structure (NMR) of the protein (Protein Data Bank code 1FYJ) was used as starting structure [19] was used as a starting structure. A single monomer was solvated with SPC water molecules in a cubic box, having an edge length of 35Å. The simulation was performed using GRONingenMACHINE for Chemical Simulation [20]. The LINCS algorithm was used to constrain all bond lengths [21]. The simulation was conducted at a constant temperature (300 K), coupling each component separately to a temperature bath using the Berendsen coupling method [22]. A cutoff of 0.9 nm was used for Lennard

Jones interaction and 1.0 nm for Coulomb interaction. The time step was 2 fs, with coordinates stored after every 4 ps. MD simulation was performed for 12ns. Before running simulation, an energy minimization was performed in steepest descent method followed by conjugate gradient method [23, 24]; and this was followed by 1.0 ns of simulation imposing positional restraints on the non-H atoms. The positional restraints were then released and 12ns production run were obtained and analyzed. Analysis programs from GROMACS were used and PCA was performed with the MD trajectory.

7.3: Results and discussion

The overall structural stability of the protein during the simulation has been monitored using several parameters like RMSD, radius of gyration (Rg), RMSF etc.

The time evolutions of RMSD of the whole protein of human bifunctional glutamyl-prolyl-tRNA during the full simulation time (Fig 1) shows an initial drift in RMSD which may be due to the difference of crystal structure with solution structure. It is evident from figure 1 that RMSD slightly increases up to 4000ps, and then slightly decreases and again increases up to 9500ps and after that almost become stable.

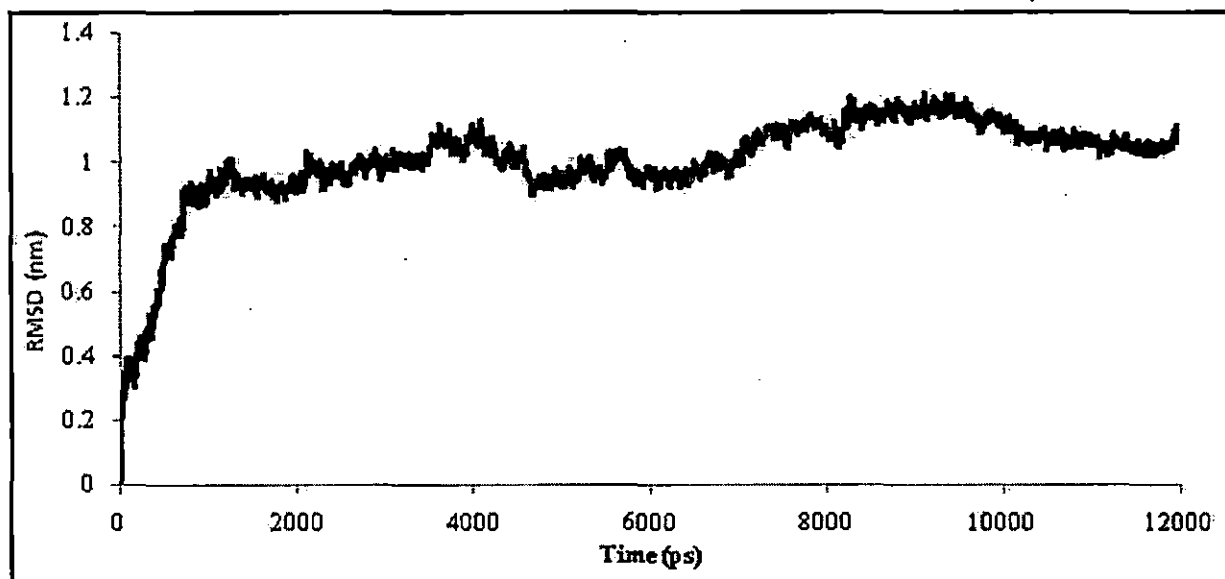


Fig 1: Time evolution of RMSD during whole simulation of time

The variation of radius of gyration (R_g) as function of time is presented in figure 2, and from this figure it is clear that R_g show much variation during the simulation time which indicates that the protein is much flexible.

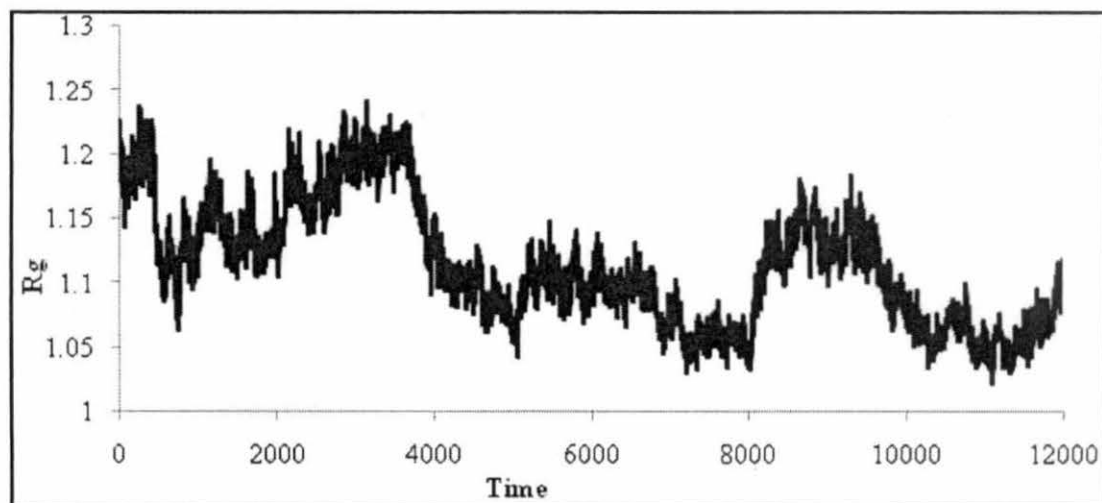


Fig 2: Time evolution R_g changes in aqueous medium during 12,000 ps Dynamics simulation

The flexibility of different segments of the protein is also revealed by looking at the root mean-square fluctuation (RMSF) of each residue from its time-averaged position. RMSF of $C\alpha$ is presented as a function of residue number in figure 3. From RMSF, it is evident that first and last residue fluctuates considerably. Interestingly pronounced fluctuations are observed for both the helices. The hydrophobic interaction between Tyr727 in the loop Tyr682, Tyr719 in the helix shows less fluctuation.

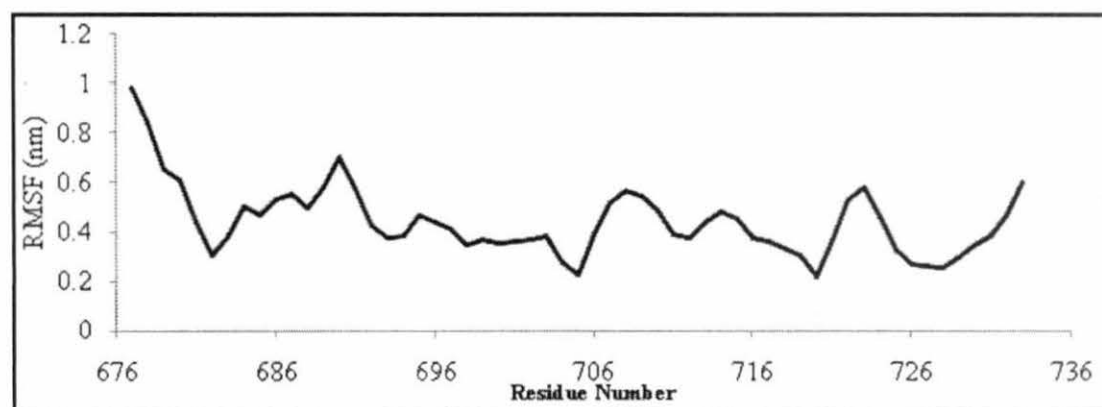


Fig 3: Plot of RMSF value of $C\alpha$ atoms value in aqueous medium presented as a function of residue number of human bifunctional glutamyl-prolyl-tRNA synthetase in starting NMR structure

The flexibility of different segments of the protein is also revealed by looking at the root mean-square fluctuation (RMSF) of each residue from its time-averaged position. RMSF of $C\alpha$ is presented as a function of residue number in figure 3. From RMSF, it is evident that first and last residue fluctuates considerably. Interestingly pronounced fluctuations are observed for both the helices. The hydrophobic interaction between Tyr727 in the loop Tyr682, Tyr719 in the helix shows less fluctuation.

RMSD of C terminal α helices, H1 and H2 are computed and presented in figure 4. It is observed that helix H1 have more fluctuations than helix H2.

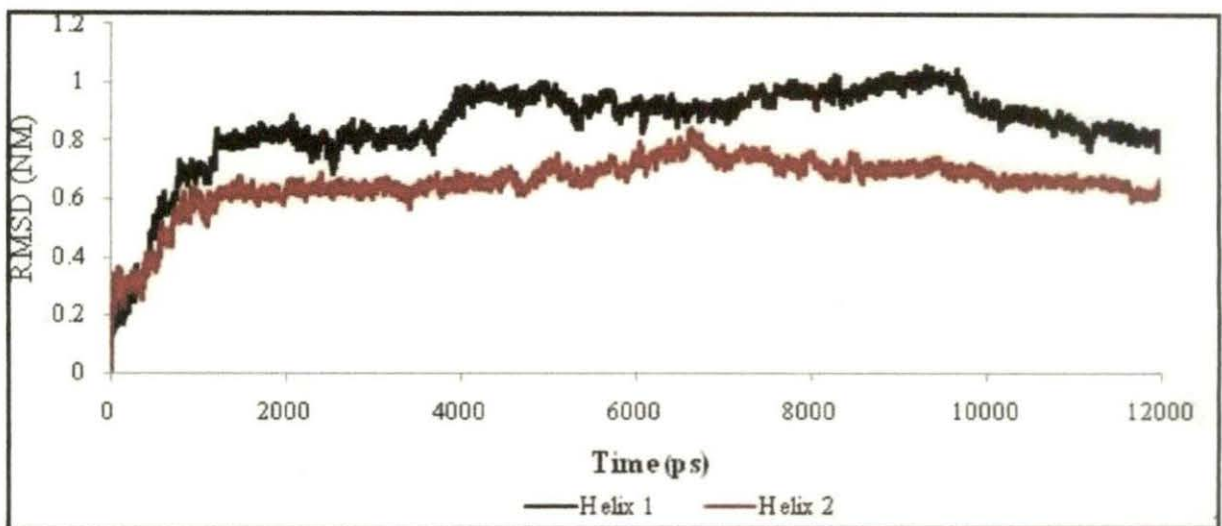


Fig 4: Plot of time evaluation of RMSD values of Helix H1 and Helix H2

A common approach in the identification of the major motions of a protein is the use of PCA [25, 26]. PCA reduces the dimensionality of a complex data set and applied to decompose a complex motion of proteins, which are characterized by an eigenvector and an eigenvalue. The eigenvalue for a given motion represents the contribution of the corresponding eigenvector to the global motion of the protein. PCA of the human bifunctional glutamyl-prolyl-tRNA synthetase simulation reveals that the first 10 eigenvectors account for 88.67% of the global motion and that the first eigenvector

corresponds to 40.46% of the total motion, the second to 13.19%, and the third to a further 11.70% (Fig 5).

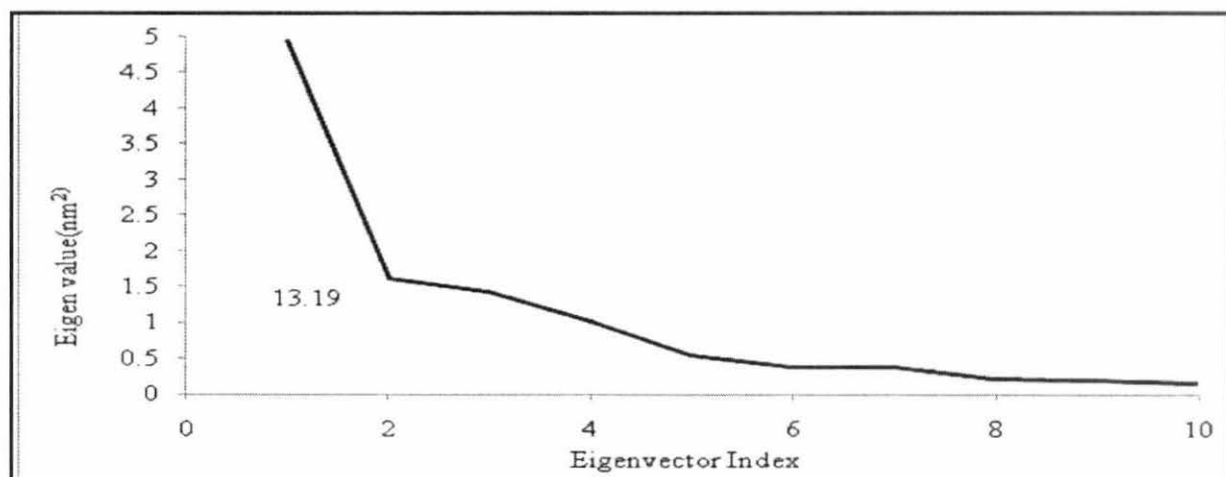


Fig 5: Plot of Eigen values with Eigenvector indices

During the simulation, several hydrogen bonds broke and formed. It is found that the number of hydrogen bonds ranged from 17 to 49 during simulation (Fig 6). The hydrogen bond network is weak, because there is a variation in number of hydrogen bonds support the molecule is flexible.

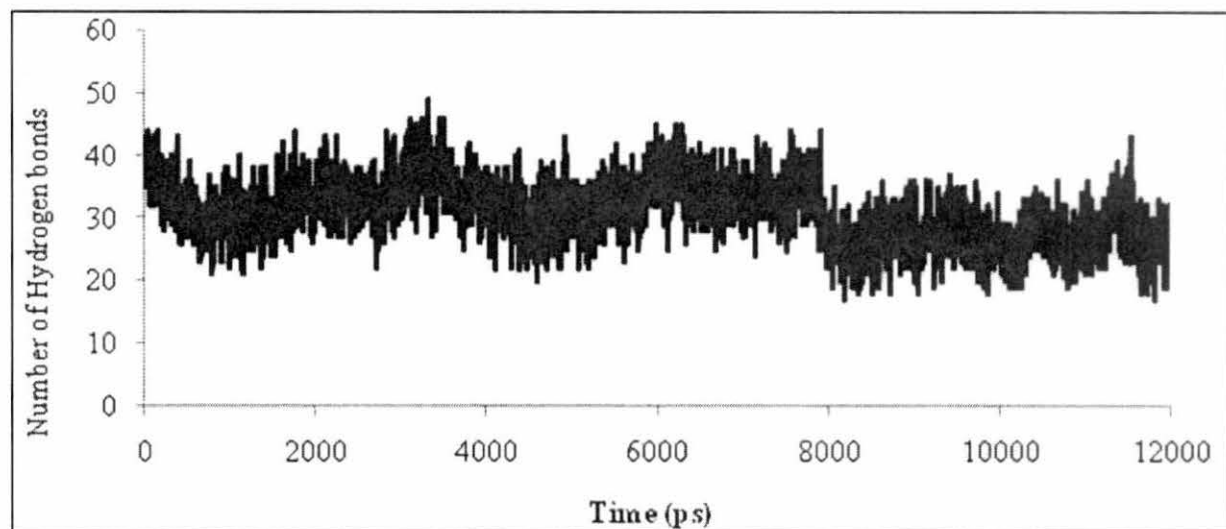


Fig 6: Number of Hydrogen bonds during the whole simulation of Time

The probability of sampling the phase space determined by first two principal modes during the simulations of the protein is presented in Figure-9. From this figure it is clear that the protein is sampling different conformational space during the simulation.

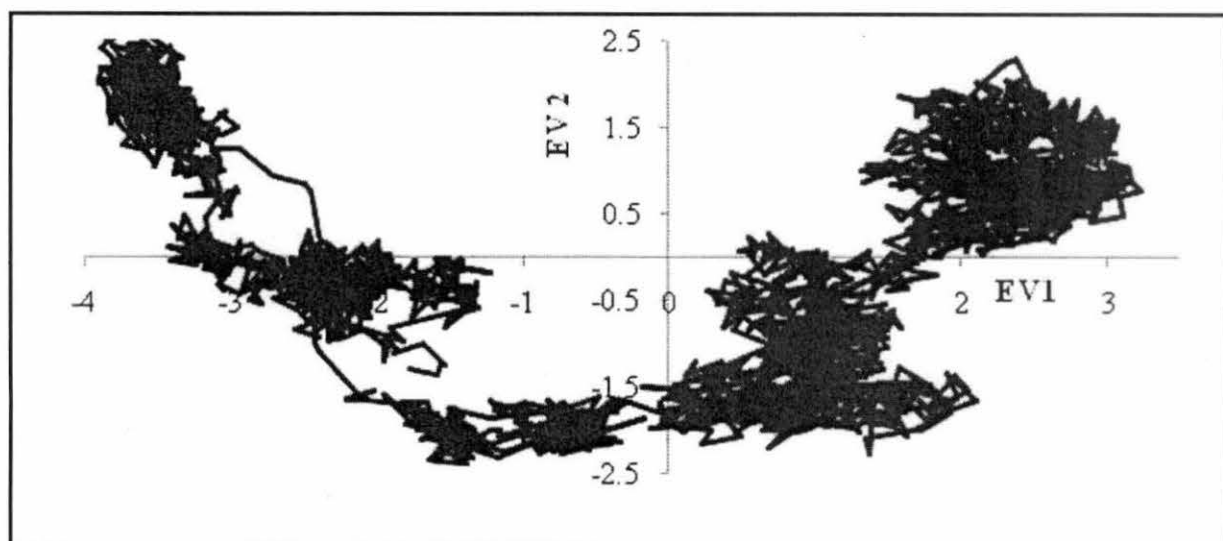


Fig 9: Plot of Eigenvector 1 with Eigenvector 2

We further examine the probability of accessing regions of the phase space determined PC1, PC2 & PC3 (Figure-10) and it is clear that the protein show very little arrangement in the XY plane and almost equally arrange in both the plane YZ and XZ.

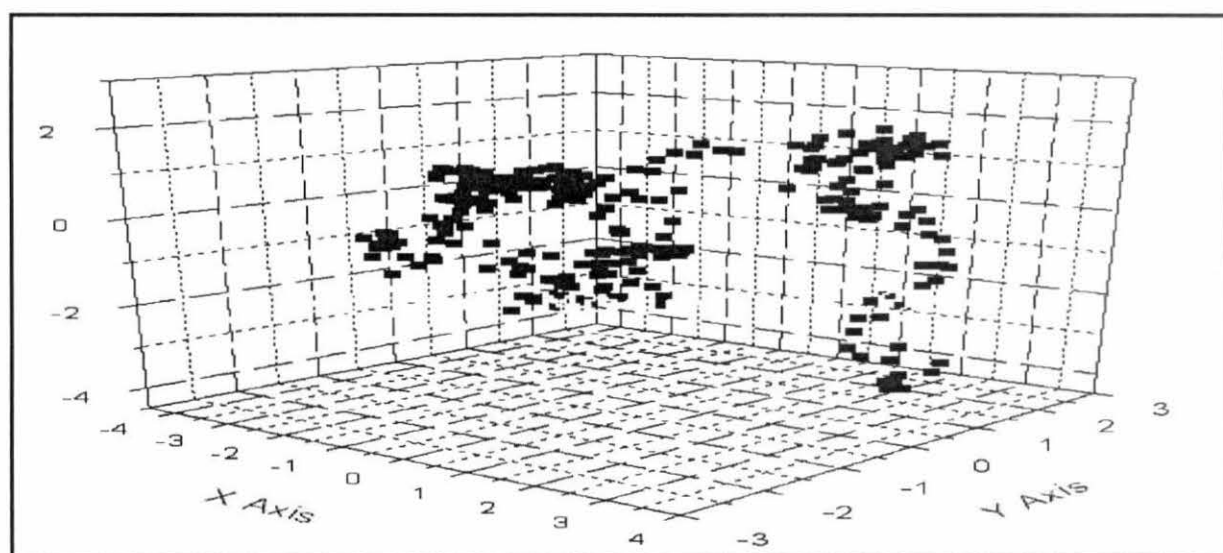


Fig 10: Conformational sampling: The Probability of sampling the phase space determined by PC1, PC2, PC3

We have taken some selected snapshots from dynamics trajectory considering time evolution of RMSD as a guideline. The snapshots were taken when the RMSD from initial structure was high, and they are presented in figure 11. From the snapshots, it is clear that there was major changes in the protein conformation which also support that the molecule is flexible.

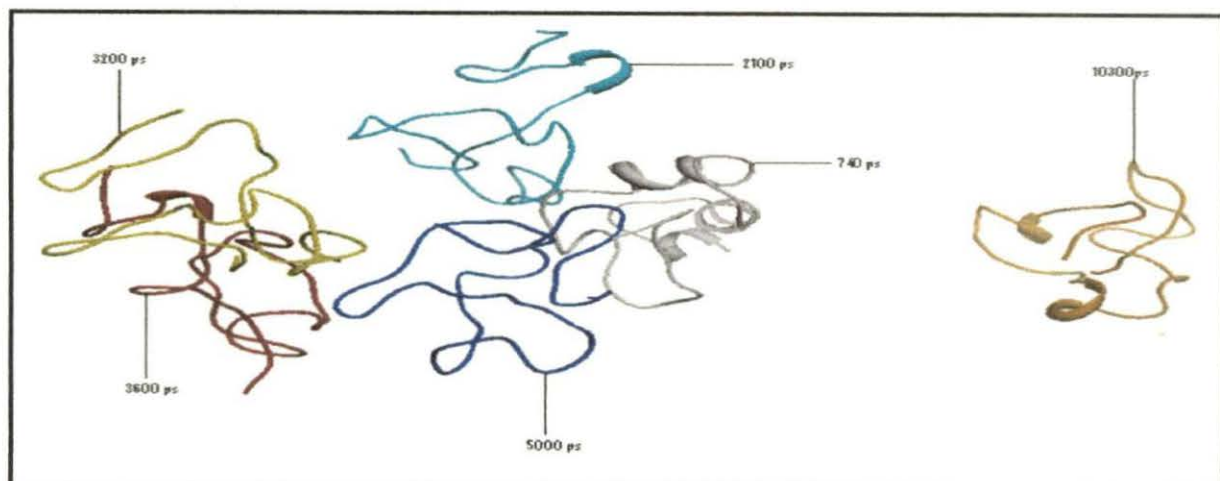


Fig 11: Snapshots at different time

From overall study it is found that during the dynamics, the structural variations, as measured by RMSD and the radius of gyration as a function time for the protein suggest that the protein is flexible.

From the probability of sampling the phase space determined by first two principal modes during the simulation the projection of the dynamics trajectory onto the first two PC that the protein traverses one conformational space around the origin and another at the right side of the origin and also at the left side of the origin which are much scattered, indicating high conformational freedom of the protein this is also revealed by different snapshots of the different structures extracted along the simulation trajectory in different times (Fig 11). It is also evident from Figure 9 that conformational freedom is more at the left side of the origin.

7.4: References

1. Mirande M (1991) Aminoacyl-tRNA synthetase family from prokaryotes and eukaryotes: structural domains and their implications. *Prog. Nucleic Acids Res. Mol. Biol.*, **40**: 95-142.
2. Dang CV, Dang CV (1986) Multienzyme complex of aminoacyl-tRNA synthetases: an essence of being eukaryotic. *Biochem. J.*, **239**, 249-255.
3. Kisselev LL, Wolfson AD (1994) The role of the anticodon in recognition of tRNA by aminoacyl-tRNA synthetases. *Prog. Nucleic Acids Res. Mol. Biol.*, **48**, 83-142.
4. Rho SB, Kim J, Lee JS, Motegi M, Kim H et al. (1999) Genetic dissection of protein-protein interactions in multi-tRNA synthetase complex. *Proc. Natl. Acad. Sci. U.S.A.*, **96**: 4488 – 93.
5. Quevillon S, Mirande M (1996) The p18 component of the multisynthetase complex shares a protein motif with the β and γ subunits of eukaryotic elongation factor. *FEBS Lett.*, **395**: 63-67.
6. Quevillon S, Argou F, Robinson JC, Mirande M (1997) The p43 component of the mammalian multi-synthetase complex is likely to be the precursor of the endothelial monocyte-activating polypeptide II cytokine. *J. Biol. Chem.*, **272**: 32573-9.
7. M Mirande; D Le Corre; JP Waller (1985) A complex from cultured Chinese hamster ovary cells containing nine aminoacyl-tRNA synthetases. *Eur. J. Biochem.*, **147**: 281-289.

8. Cerini C, Kerjan P, Astier M, Gratecos D, Mirande M, et al. (1991) A component of the multisynthetase complex is a multifunctional aminoacyl-tRNA synthetase. *EMBO J.* **10**: 4267-4277.
9. R Fett, R Knippers (1991) The Primary Structure of Human Glutaminyl-tRNA Synthetase. *J. Biol. Chem.*, **266**, 1448-1455.
10. Heacock D, Forsyth CJ, Shiba K, K Musier-Forsyth K (1996) Chemical Modification and Site-Directed Mutagenesis of the Single Cysteine in Motif 3 of Class II *Escherichia coli* Prolyl-tRNA Synthetase. *Bioorg. Chem.*, **24**, 273-289.
11. Nada S, Chang PK, Dignam JD (1993) Primary structure of the gene for glycyl-tRNA synthetase from *Bombyx mori*. *J. Biol. Chem.*, **268**: 7660-7667.
12. Shiba K, Schimmel P, Motegi H, Noda T (1994) Human glycyl-tRNA synthetase. Wide divergence of primary structure from bacterial counterpart and species-specific aminoacylation. *J. Biol. Chem.*, **269**: 30049-30055.
13. Frolova LY, Sudomoina
MA, Grigorieva AY, Zinovieva OL, Kisselev LL (1991) Cloning and nucleotide sequence of the structural gene encoding for human tryptophanyl-tRNA synthetase. *Gene*, **109**: 291-296.
14. Lee CC, Craigen WJ, Muzny DM, Harlow E; Caskey CT (1990) Cloning and nucleotide sequence of the structural gene encoding for human tryptophanyl-tRNA synthetase. *Proc. Natl. Acad. Sci. U. S. A.*, **87**: 3508-3512.
15. Tsui FW, Siminovitch L (1987) Isolation, structure and expression of mammalian genes for histidyl-tRNA synthetase. *Nucleic Acids Res.*, **15**: 3349-3367.

16. HirakantM,SuwaA, TakedaY, MatsuokaY,IrimajiriS, et al. (1996) *J Craft. Arthritis Rheum.*,39, 146-151.
17. Craft J. *Arthritis Rheum.*,1996, 39, 146-151.
18. RabenN, NicholsR,DohlmanJ,McphieP, SridharV (1994) C Hyde; R Leff; P Plotz. A Motif in Human Histidyl-tRNASynthetase Which Is Shared among SeveralAminoacyl-tRNASynthetases Is a Coiled-coil That Is Essential for Enzymatic Activity and Contains the Major AutoantigenicEpitop. *J.Biol. Chem.*,269, 24277-24283.
19. RhoSB, LeeJS,JeongEJ,KimKS, KimYG, et al. (1998)A multifunctional repeated motif is present in human bifunctionaltRNAsynthetase.*J.Biol.Chem.*,273: 11267-11273.
20. JeongEJ, HwangGS, KimKH, KimMJ, KimS (2000) KS Kim.Structural Analysis of Multifunctional Peptide Motifs in Human BifunctionaltRNAsynthetase: Identification of RNA-Binding Residues and Functional Implications for Tandem Repeats. *Biochemistry*.39: 15775-15782.
21. Lindahl E, Hess B, et al. (2001) GROMACS 3.0: A package for molecular simulation and trajectory analysis. *J. Mol. Model.*, 7: 306-317.
22. Berendsen HJC, Postma JPM *et al.* (1984) Molecular dynamics with coupling to an external bath.*J. Chem. Phys* 81: 3684–3690.
23. Essmann U, Perera L, et al. (1995) A smooth particle mesh Ewaldmethod. *J. Chem. Phys.*, 103(19): 8577–8593.
24. AK Bothra; S Roy; B Bhattacharya; C Mukhopadhyay. *Journal of Biomolecular and Dynamics*.1998, 15(5), 999-1008.